JOURNAL OF THE MECHANICAL BEHAVIOR OF BIOMEDICAL MATERIALS 51 (2015) 215–224

Available online at www.sciencedirect.com

ScienceDirect

www.elsevier.com/locate/jmbbm



Research Paper

Effect of Zr, Nb and Ti addition on injection molded 316L stainless steel for bio-applications: Mechanical, electrochemical and biocompatibility properties

H. Ozkan Gulsoy[a,*], Serdar Pazarlioglu[a], Nagihan Gulsoy[b], Busra Gundede[c], Ozal Mutlu[b]

[a]Marmara University, Technology Faculty, Metall. and Mater. Eng., 34722 Istanbul, Turkey
[b]Marmara University, Faculty of Arts and Sciences, Department of Biology, 34722 Istanbul, Turkey
[c]Marmara University, Institute of Pure and Applied Sciences, 34722 Istanbul, Turkey

ARTICLE INFO

Article history:
Received 30 April 2015
Received in revised form
14 July 2015
Accepted 17 July 2015
Available online 26 July 2015

Keywords:
Powder injection molding
Sintering
Corrosion resistance
Biocompatibility

ABSTRACT

The research investigated the effect of Zr, Nb and Ti additions on mechanical, electrochemical properties and biocompatibility of injection molded 316L stainless steel. Addition of elemental powder is promoted to get high performance of sintered 316L stainless steels. The amount of additive powder plays a role in determining the sintered microstructure and all properties. In this study, 316L stainless steel powders used with the elemental Zr, Nb and Ti powders. A feedstock containing 62.5 wt% powders loading was molded at different injection molded temperature. The binders were completely removed from molded components by solvent and thermal debinding at different temperatures. The debinded samples were sintered at 1350 °C for 60 min. Mechanical, electrochemical property and biocompatibility of the sintered samples were performed mechanical, electrochemical, SBF immersion tests and cell culture experiments. Results of study showed that sintered 316L and 316L with additives samples exhibited high corrosion properties and biocompatibility in a physiological environment.

© 2015 Elsevier Ltd. All rights reserved.

1. Introduction

Over the years, material research has led to development of numerous metals and alloys use in biomedical applications (Breme et al., 2007; Zhao et al., 2015; Auzene et al., 2014). Besides stainless steel plays an important role, due to its corrosion resistance and excellent mechanical properties. 316L has widespread, especially in medical and food industries (Bayraktaroglu et al., 2012). Its scope of application ranges from clinical devices such as stents and artificial joints to surgical tools. Some major tasks for biomaterial research are the functionalization of the material surface, ingredients, corrosion to improve the biocompatibility according to specific applications. However, the correlation between material properties and the reaction of a biological system is usually very complex (Elter et al., 2009; Wang et al., 2015). One the first events that takes place when a

*Corresponding author. Tel.: +90 216 3365770 1322; fax: +90 216 3378987.
E-mail address: ogulsoy@marmara.edu.tr (H.O. Gulsoy).

http://dx.doi.org/10.1016/j.jmbbm.2015.07.016
1751-6161/© 2015 Elsevier Ltd. All rights reserved.

foreign material comes into contact with a living body is biocompatibility. This depends on corrosion of material, material surface properties, ingredients and topography (Li et al., 2014).

Powder injection molding (PIM) is a manufacturing technology for the net-shape production of small, intricate, and precise metallic and ceramic parts and components. The PIM process includes mixing of powders with a binder to produce a feedstock; injection molding to form a green part with the desired shape by making the feedstock flow into and fill a mold under pressure; debinding to form a brown part by removing the binder components, and finally sintering to near full density. The process overcomes the shape limitation of traditional powder compaction, the cost of machining, the productivity limits of isostatic pressing and slip casting, and the defect and tolerance limitations of conventional casting (German and Bose, 1997; Gulsoy et al., 2007; Gulsoy, 2005; Zhao et al., 2015).

In recent years, the interest in PIM for stainless steel alloys such as 316L, 17-4PH and 430 and their alloy parts for general use (household, automotive, dental, biomedical, military and aerospace) has dramatically increased (Gulsoy, 2005), as evidenced by the number of scientific papers and successful use-oriented developments. Stainless steel alloys have been investigated due to their attractive properties, such as specific strength with good ductility, excellent surface properties, corrosion resistance and

Table 1 – Powder characteristic of 316L, Zr, Nb and Ti powder.

Item	316L	Zr	Nb	Ti
Vendor	Osprey Metals	Alfa Aesar	Alfa Aesar	Alfa Aesar
Shape	Spherical	Irregular	Irregular	Irregular
Theoretical density, g/cm^3	7.96	6.51	8.57	4.50
Particle size				
D_{10}	4.41	1.95	3.01	2.35
D_{50}	12.01	6.97	8.21	7.81
D_{90}	27.70	26.72	25.62	30.2
Purity, %	–	99.9	99.9	99.9

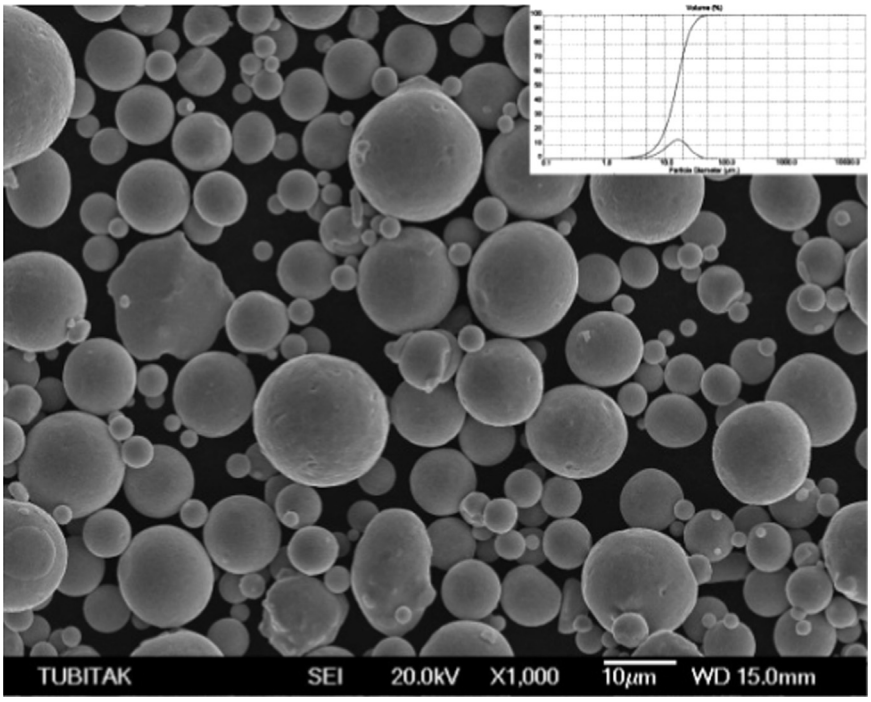


Fig. 1 – Scanning electron micrograph of 316L powder and particle size distribution curve.

Table 2 – Ion concentrations of the SBF and human blood plasma (mmol/L).

Sample	Na^+	K^+	Ca^{2+}	Mg^{2+}	HCO_3^-	Cl^-	HPO_4^{2-}	SO_4^{2-}
Blood plasma	142.0	5.0	2.5	1.5	27.0	103.0	1.0	0.5
SBF	142.0	5.0	2.5	1.5	4.2	147.8	1.0	0.5

average density compared to other materials (German and Bose, 1997). 316L alloys in stainless steel family have an average density, relatively high strength and excellent corrosion resistance in many media and are known to be biocompatible (Bayraktaroglu et al., 2012). These materials can be easily produced by conventional powder metallurgy processing, but a major problem to be overcome in the conventional powder processing is the oxide film and residual radical elements such as C, O and N (Bayraktaroglu et al., 2012; Gulsoy, 2005; Nakamura et al., 2011; Hong et al., 2005; Suri et al., 2005). Oxides, nitrides and sulfur on surfaces of powder prevents to high densification at sintering stages. These problems form a large barrier for sintering behaviors and the final properties of 316L alloys. In general, 316L powder can be sintered by solid-state sintering technique. Some elemental additives such as Zr, Nb and Ti in starting 316L powder can trap oxides on powder surfaces (Parsapour et al., 2013). As a result of this, it may be possible high corrosion properties and biocompatibility for final sintered parts.

The present research investigates the effect of Zr, Nb and Ti additions on mechanical electrochemical properties and biocompatibility of injection molded 316L stainless steels. Metallographic and mechanical test techniques were employed for the sintered samples to investigate the microstructural development and mechanical properties. The sintered samples were characterized for their corrosion resistance in two different environments an acid solution (0.5 M H_2SO_4) and SBF using potentiodynamic polarization. Bioactivity of the all samples in a SBF was investigated. Surface of samples after SBF treatment and proliferation of cells were analyzed under scanning electron microscope (SEM). Cell viability tests were carried out by MTT assay, ROS assay and Trypan Blue-Dye exclusion analysis.

2. Experimental procedures

2.1. Test materials and fabrication method

In this research, gas atomized 316L stainless steel powders (Fe–17Cr–12Ni–2.5Mo–1Si–2Mn–0.03C–0.045P–0.003S) provided by Osprey Metals Ldt. was used to prepare the samples. The Ti, Nb and Zr powder was obtained from Alfa Aesar. Particle size distributions of all powder were determined on Malvern Mastersizer equipment and given in Table 1. Morphology of the 316L powder was examined using scanning electron microscopy and

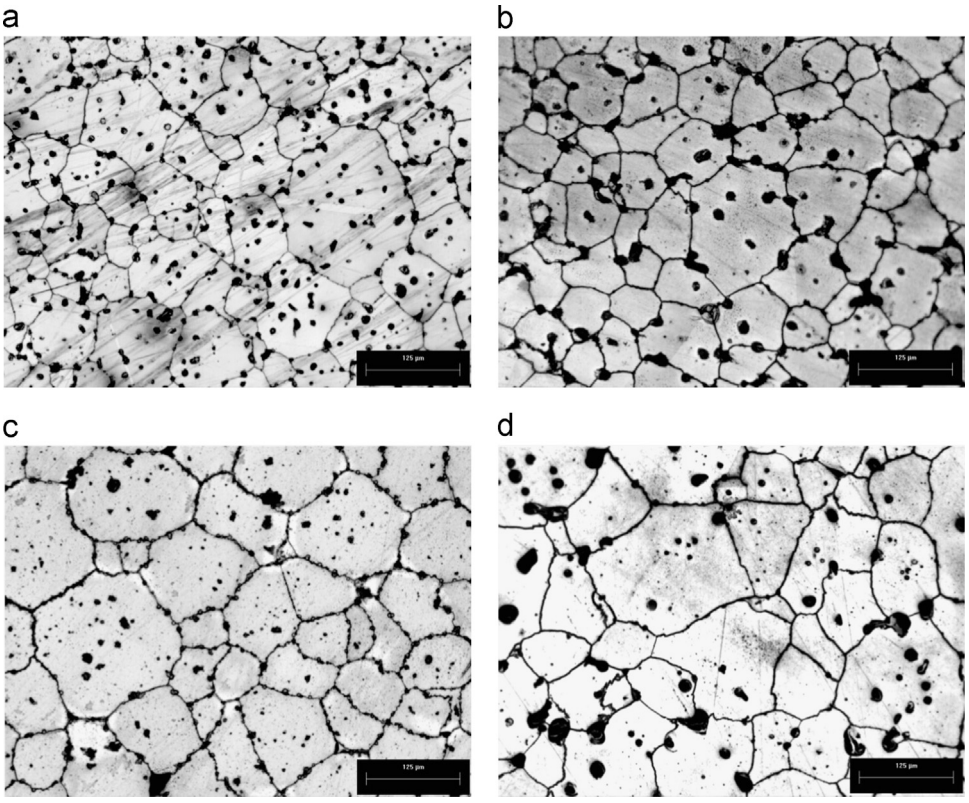


Fig. 2 – Optical micrographs of 316L and 316L additions samples sintered at 1350 °C: (a) 316L, (b) 0.75 Zr, (c) 0.75 Nb and (d) 0.75 Ti.

Table 3 – Mechanical properties of sintered 316L stainless steels with and without additions.

Samples	316L	316L 0.75 Zr	316L 0.75 Nb	316L 0.75 Ti
Density, g/cm^3	7.2	7.4	7.4	7.2
Tensile strength, MPa	370	403	463	475
Hardness, HRA	43	53	51	53

given in Fig. 1. The gas atomized 316L stainless steel powder is spherical in shape and additive powder is irregular in shape.

The amount of additives was given 0.75 wt% in starting mixture and each mixture was blended in a Turbula mixer for five hours. A multiple-component binder system consisting of paraffin wax (69 wt%), polypropylene (10 wt%), carnauba wax (20 wt%), and stearic acid (1 wt%) was employed. Feedstock was prepared at 175 °C with the binder melted first and then powder blend added incrementally. The powder loading in this mixture was 62.5 vol% (Gulsoy et al., 2007). After cooling, the feedstock was pelletised by hand. These feedstocks were injected using a 12.5 MPa tailor-designed injection-molding machine to produce test samples. Debinding was performed in a two-step solvent/thermal operation. Green parts were solvent debound at 60 °C for 5 h in heptanes (Gulsoy et al., 2007; Gulsoy, 2008), followed by thermal debinding step at slow heating rate in high purity hydrogen atmosphere. Sintering of all samples was performed in an atmosphere-controlled high temperature furnace. The sintering cycle was as follows: samples were heated to sintering temperatures of 1350 °C at a rate of 5 °C/min and they were held at sintering temperature for 60 min in high purity hydrogen atmosphere.

2.2. Physical and mechanical tests

The densities of the sintered samples were measured by means of the Archimedes water-immersion method. For metallographic examination, the samples were cut from the tensile bars, polished to a 0.3 μm surface finishing using standard metallographic procedures. Polished samples were etched for optical metallography.

All tensile tests were performed using Zwick 2010 mechanical tester at a constant crosshead speed of 1 mm/min (25 mm gauge length). The hardness tests were performed using an Instron-Wolpert Dia Testor 7551 at HRB scale. The fracture surfaces were examined using a scanning electron microscope (Jeol-JSM 6335F). Five samples were tested under the same conditions to guarantee the reliability of the results. At least three samples were tested under the same conditions for the reliability of the results.

2.3. Electrochemical tests

For electrochemical evaluation, the cylindrical samples were polished to mirror finish in alcohol. The potentiodynamic scans were conducted using a flat cell, supplied by Gamry Instruments at room temperature. A standard three-electrode (reference, counter and working) technique was used for the measurement. The reference electrode used for the present experiment was saturated calomel electrode and the sintered alloy was chosen as the working electrode. The exposed area of the sintered sample to the solution was 8.03 mm^2. The electrochemical experiments were performed using a PC controlled Gamry Echem Analyst system software. Prior to the polarization test, each sample was stabilized for about the solution to get a stable open circuit potential (OCP). The potentiodynamic polarization tests were conducted minimum of three times at a constant scan rate of 1 $mV\,s^{-1}$ in freely aerated 0.5 M H_2SO_4 and SBF. The potentiodynamic

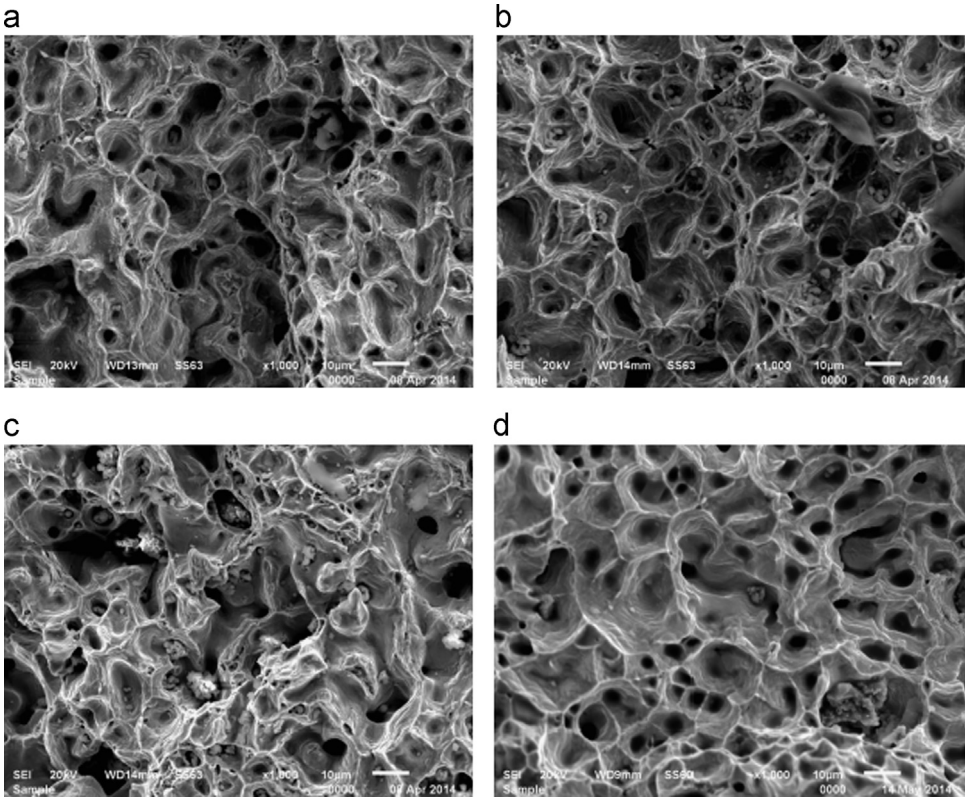


Fig. 3 – SEM fractographs of with and without additive at 1350 °C for 60 min, (a) 316L, (b) 0.75 wt% Zr, (c) 0.75 wt% Nb and (d) 0.75 wt% Ti.

scan of sample was given in graphical form (voltage versus current density). The Tafel slopes were established from the active region of the corresponding anodic and cathodic curves. The critical parameters like corrosion potential (Ecorr), corrosion current (Icorr) and corrosion rate were evaluated from the polarization curves.

2.4. *In vitro and cell culture tests*

The sintered samples with a size of $\varnothing 15 \times 5\ mm^2$ were prepared for SBF and cell culture tests. The samples as prepared were polished by rough sand paper and rinsed ultrasonically in acetone, absolute alcohol and deionized water in turn for five times. Finally, they were dried in an oven at 70 °C for 24 h. The samples were obtained for investigation in SBF. The special preparation process of SBF was as follows. The solution was prepared by dissolving reagent grade sodium chloride (NaCl), potassium chloride (KCl), calcium chloride dihydrate ($CaCl_2 \cdot 2H_2O$), magnesium chloride hexahydrate ($MgCl_2 \cdot 6H_2O$), sodium hydrogen carbonate ($NaHCO_3$), dipotassium hydrogen phosphate trihydrate ($K_2HPO_4 \cdot 3H_2O$), sodium sulfate (Na_2SO_4) in deionized water. Then the solution was buffered to physiological pH 7.4 at 37.5 °C by both hydrochloric acid (HCl) and tris (hydroxymethyl)-aminomethane ($(CH_2OH)3CNH_2$) (Xin et al., 2009). The ion concentration of the SBF is shown in Table 2. The sintered samples were immersed in sealed test tubes containing 20 ml of SBF for 3, 7, 15 and 30 days. The experiment was performed in a laboratory water bath that was maintained at a constant temperature of 37.5 °C and subjected to a continuous vibrating motion to help maintain uniform ion concentration. After immersion in SBF for various periods, the sintered samples were retrieved, gently rinsed with distilled water, and dried at 45 °C for 1 day. After drying the samples were sputter coated with Au for SEM observation. The surface of the samples was finally examined by SEM.

For cell culture tests, 3T3 mouse embryonic fibroblast cell line was provided by American Type Culture Collection (Rockville, MD, USA) and was grown in monolayer culture in Dulbecco's Modified Eagle's Medium (Gibco, Milan, Italy) supplemented with 10% heat-inactivated fetal bovine serum (Gibco, Milan, Italy), and 1% penicilin–streptomycine antibiotic mixture (Gibco, Milan, Italy) at 37 °C with 5% CO_2 and 95% humidity. Trypsin/EDTA 0.25% solution was used to remove cells from the culture flask. Cells were reseeded at a density of 1×10^5 cells into the 25 T flasks. Culture medium change took place every 3 days. For SEM analysis, alloy samples and glass coverslip (negative control) were placed in to the 6-wells culture plates containing of 5 ml complete DMEM medium

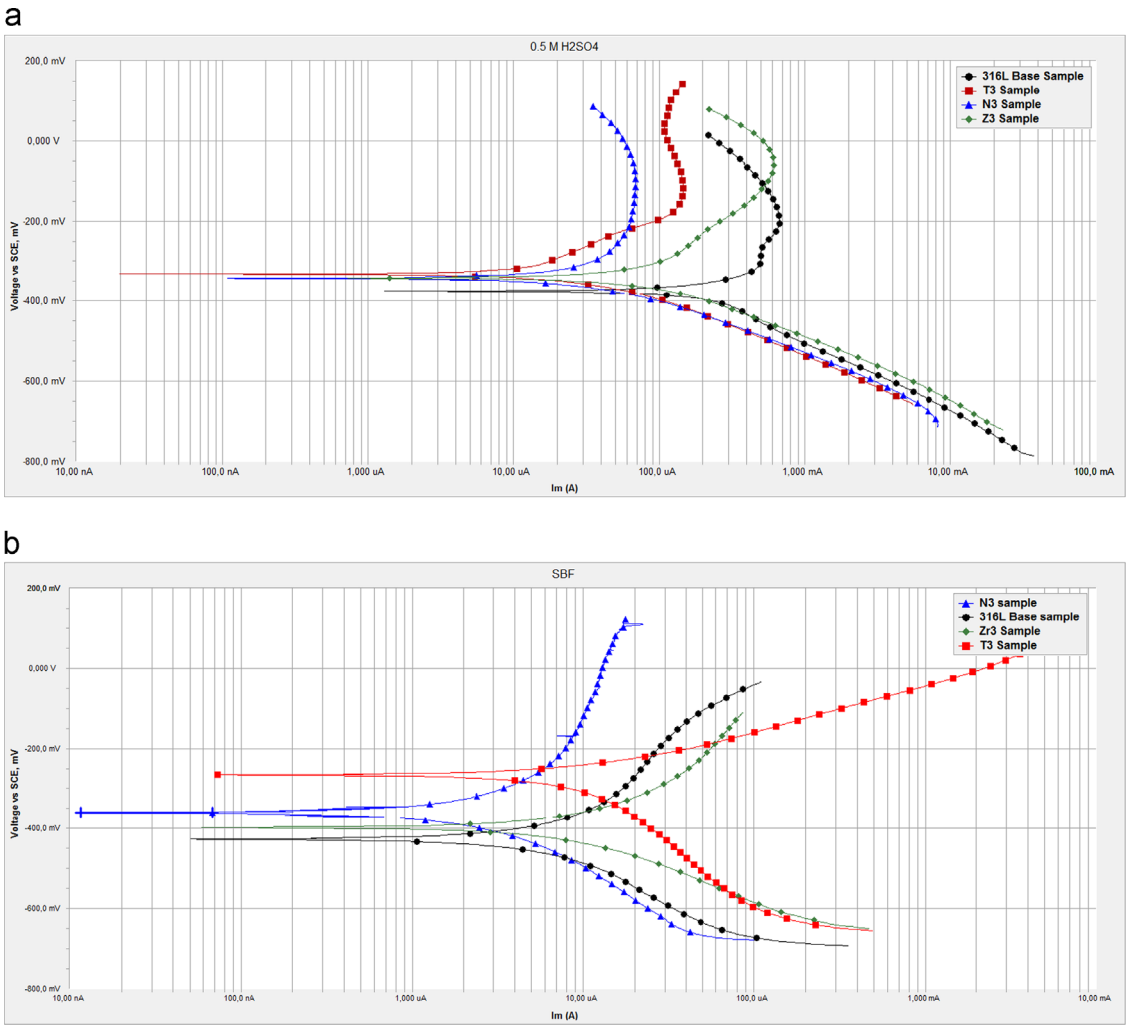


Fig. 4 – Tafel curves for the 316L and 316L-additions samples sintered at 1350 °C: (a) 0.5 M H_2SO_4, (b) SBF media.

and then 3T3 cells were seeded with the concentration of 5×10^4 cells/well for 96 h. After treatment medium was removed, samples were washed with 0.15 M PBS buffer and fixed with 2.5% gluteraldehyte (4 °C). Samples were treated with 1% osmium tetroxide as secondary fixation, dehydrated with aceton series and incubated in amyl acetate. The glass coverslip and samples were critical-point dried and mounted on appropriate stubs with carbon tape and sputter-coated with gold. Images were collected using a SEM. All samples were analyzed for twice.

Trypan blue-dye exclusion test was used to determine cell viability. Cell viability is calculated as the number of viable cells divided by the total number of cells within the grids on the cell counter (BioRad TC10) which counted the number of blue staining cells and the number of total cells. Cell viability should be at least 95% for healthy log-phase cultures (Elter

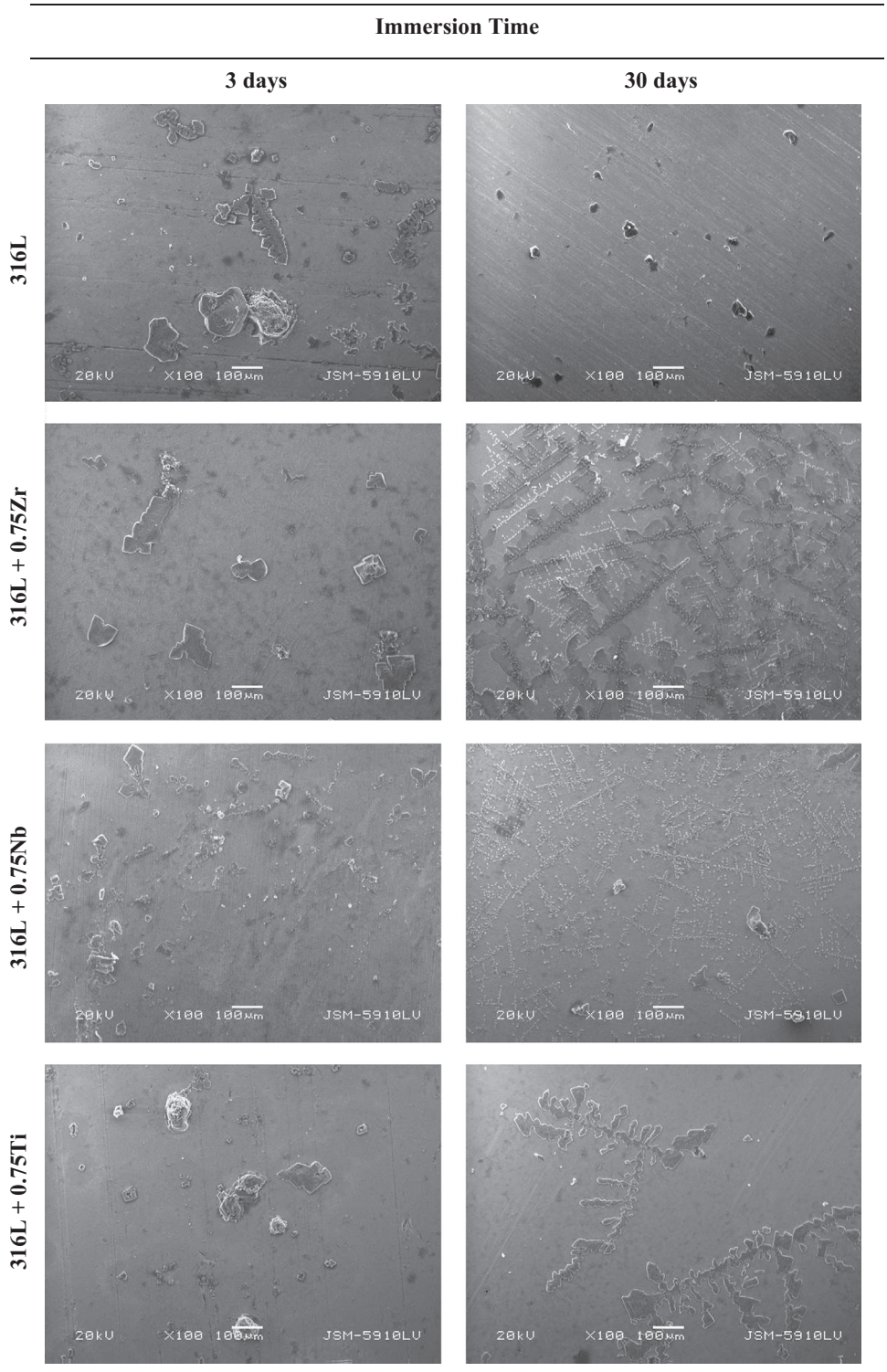


Fig. 5 – SEM morphologies of the surfaces of sintered 316L and 316L-additions samples for 3 and 30 days immersion in SBF.

et al., 2009). For MTT (3-(4.5-dimethylthiazol-2-yl)-2,5-diphenyltetrazolium bromide) assay, cells were cultivated in 6-well flask within 5 ml DMEM and incubated in the same conditions as stated above. The MTT substrate is prepared in a physiologically balanced solution, added to cells in culture at a final concentration of 0.5 mg/ml, incubated for 4 h and then acid-isopropanol was added for solubilize to formazan crystals. The detection of cell vitality is based on the reduction of a yellow colored dye MTT to the blue-violet formazan. The quantity of formazan (presumably directly proportional to the number of viable cells) is measured by recording changes in absorbance at 570 nm using a plate reading spectrophotometer (Epoch, Biotek, USA). Reactive oxygen species (ROS) were determined by staining the cells with DFCDA (2′,7′-Dichlorodihydrofluorescein diacetate, Sigma) dye which shows fluorescence feature when reacts with reactive oxygen species. Cell were grown for 96 h, ROS solution added on cells in 6-well plate flasks and incubated for 1 h. and observations were made under a fluorescence microscope (Olympus BX51) using an image analysis system (Kameram, Micro System Ltd. Turkey). Fluorescence signal indicates ROS generation by cells (Elter et al., 2009). All of the results were analyzed using One Way Anova.

3. Results and discussion

3.1. *Microstructure and mechanical properties*

Fig. 2 shows the optical micrographs of 316L samples with and without additions sintered for 60 min at 1350 °C. From Fig. 2 it is evident that 316L stainless steels sintered for 1350°C have significantly lower porosity. Sintering results in improved sintered density in all straight 316L as well as 316L-additions samples. Ti added samples present lower density than that of 316L stainless steel at all sintering temperatures, for two reasons. The first reason is the lower density of the additions that reduces the density of the sintered samples. The second reason is that added particles impede the sintering process. Result of density shows that at sintering temperature 1350 °C and sintering time 60 min, 316L samples attained a maximum density of 7.2 g/cm^3. In 0.75 wt% Nb, Zr and Ti added samples at sintering temperature 1350 °C and sintering time 60 min, attained a maximum density of 7.4, 7.4 and 7.2 g/cm^3, respectively. The densities of all samples were increased Nb, Zr and Ti additions. However, Ti additions caused a decrease in the density of samples. This result shows that the two types of additions improve the density of samples. On the other hand, microstructure of Nb and Ti added samples exhibited coarse compare to 316L and Zr added samples. Additions led to lower grain growth but the amount of porosity is significantly reduced. Especially, amount of pores in grain decreased and pores recovered on grain boundary for Nb and Ti added samples. The diffusion rate and amount of additions are important for microstructural evolution and final properties (German, 1996; Nakamura et al., 2011). In Ti added samples, more and larger pores are present at the grain boundaries. As a result, size grain was increased very little and sintered density was decreased for Ti added samples (Shaw, 1989; Dehoff et al., 1966).

The effect of three type additions on the mechanical properties of 316L stainless steel is shown in Table 3. 316L

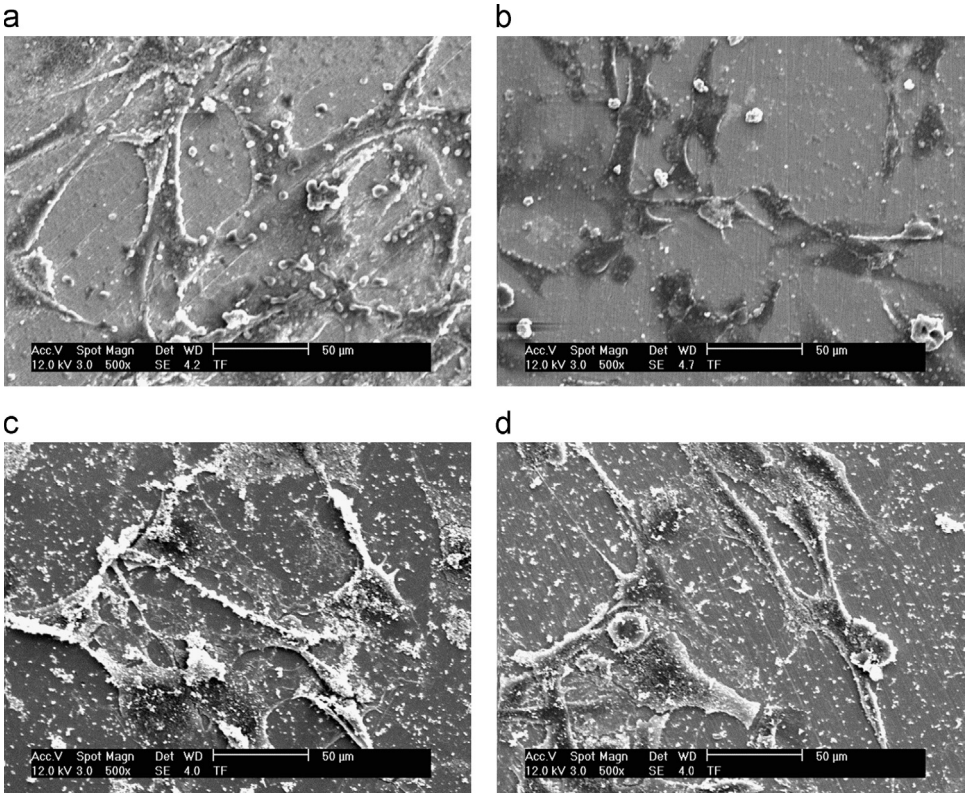


Fig. 6 – SEM micrographs cell morphology after 96 h of culture on sample surfaces: (a) 316L, (b) 0.75 Zr, (c) 0.75 Nb and (d) 0.75 Ti.

stainless steel presents good mechanical properties, especially tensile strength lower than that of added samples. The ultimate tensile strength was increased with additions. Thus, pores are closed and densities increased at high sintering temperatures. In added samples, ultimate tensile strength was increased compared to base samples, but in more additions samples (Zr 0.75%), ultimate tensile strength was decreased. In Ti added samples, density values increased slightly despite tensile strength and hardness values was increased. Ti element can easily create intermetallics and ceramics as like TiNi, TiC and TiN. Although the amounts of these phases are low level and their high hardness, tensile strength of samples can be increased (Gulsoy, 2008; Velasco et al., 2002). The effect of additions on the hardness of 316L stainless steel is shown in Table 3. The 316L with Nb, Zr and Ti addition also shows an increase in hardness. This can be rationalized in terms of the enhanced hardness in 316L additions alloys. The change in hardness can be explained by the presence of nano-size hard phases (ZrC, TiC, TiNi, NbC) in microstructures (Nakamura et al., 2011; Park et al., 2014).

Fig. 3 shows the fracture surfaces of the samples. For all samples, main fracture mode is the separation of particles and necking areas where bonding between particles took place during sintering. From Fig. 3, they are evident that

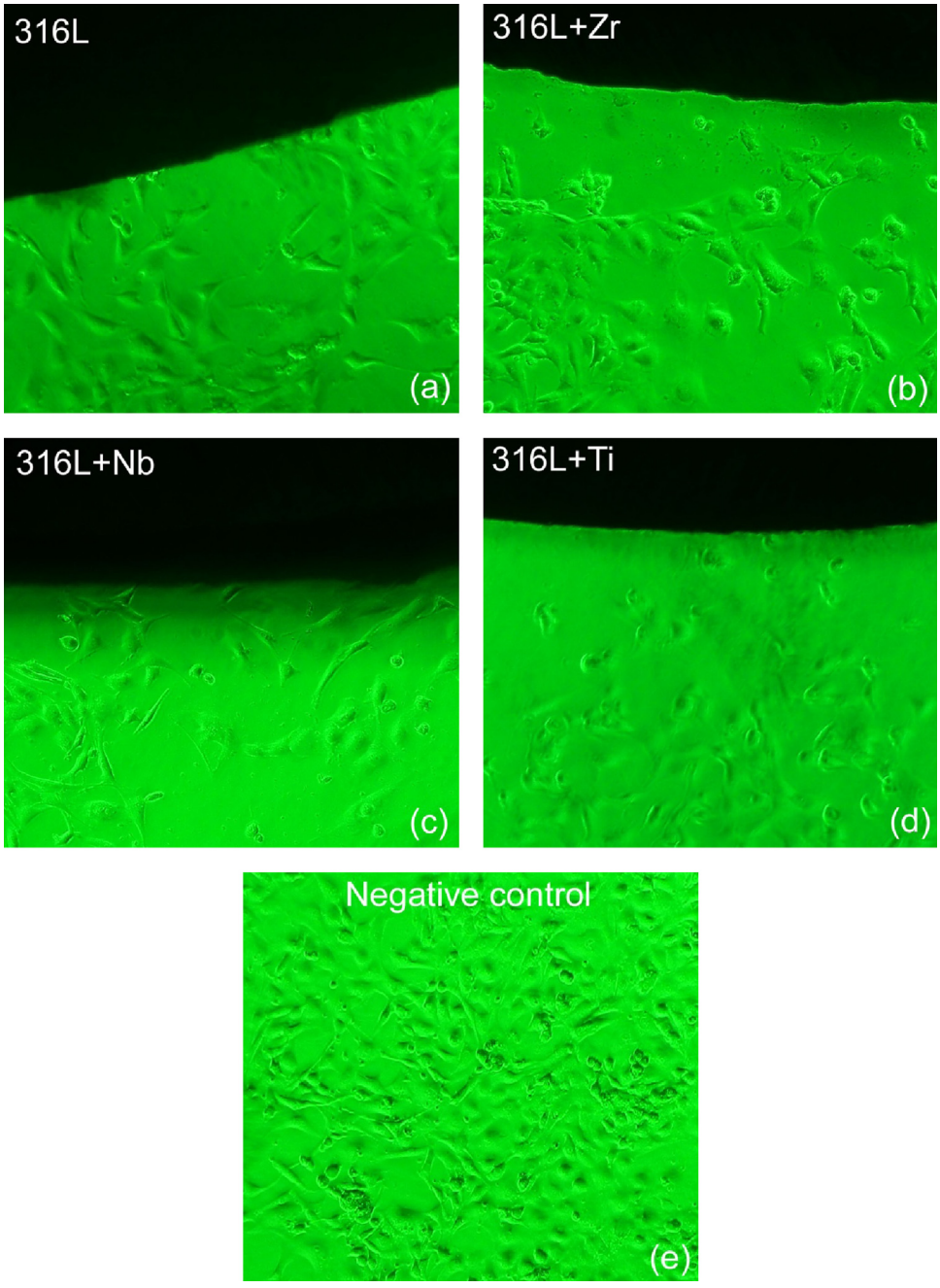


Fig. 7 – Phase-contrast micrographs of fibroblasts (black arrows) cultured for 96 h on biomaterials: (a) 316L, (b) 316L+Zr, (c) 316L+Nb (d) 316L+Ti and (e) negative control (without material).

straight 316L samples show dimpled morphology, which is indicative of ductile fracture. In added samples, fracture mode from dimpled to intergranular mode.

3.2. *Electrochemical properties*

Fig. 4 shows the extrapolation of the Tafel curves the corrosion potential, Ecorr (measured relative to SCE), Tafel slopes in the anodic and cathodic region and corrosion current density (icorr) were determined. Irrespective of the additive is a significant improvement in the corrosion resistance for the sintered samples. This can be attributed to the enhanced densification achieved by the 1350 °C sintered samples. In additions, Zr, Nb and Ti additives improved the corrosion resistance. The addition of 0.75 wt% Ti to 316L stainless steels more improves the corrosion resistance in both sintered samples. According to Tafel curves in SBF, corrosion rate of 316L with Zr, Nb and Ti is less than 316L sample. The environment constituted by the acid solution is more aggressive for stainless steel than the SBF solution. 316L with additives samples show low corrosion rate in each environment. Considering that using stainless steel in acid and SBF environment, these results are suitable for acid environments and bio-applications.

3.3. *SBF immersion and cell culture tests*

SEM morphologies of the sample surfaces after immersion in the SBF for various times are shown in Fig. 5. It can be seen that after 3 days immersion, many globular apatite particles have grown on the surface of the samples. The nucleation of the apatite prefers to occur in pores or scratch, where the size of the apatite particles is obviously much larger than that on the smooth part of the surface. With the increase of immersion time, the quantity and size of the apatite particles increase gradually. After 30 days immersion, the surface of the samples can be more covered with apatite (Tang et al., 2006; Faghihi et al., 2012; Liu and Zheng, 2011). In the initial immersion in SBF, Ca and P ions on the biocomposite surfaces are dissolved into SBF; however, the supersaturation of Ca and P ions is low. Therefore, the apatite layer is nucleated where the local ion concentrations are high comparatively and few crystal nuclei are formed. The crystal nuclei adsorb the ions from their own surrounding environment and develop in their growth process (Liu and Zheng, 2011).

Fig. 6 shows the morphologies of the cells on samples after 96 h of culture. Cells were flattened and well spread across the 316L and 316L-additions sample surfaces after 96 h, as shown in Fig. 6a and b. On both of sample surfaces, cells were seen to adhere to surface (e.g. filopodia), and were connected to the substrate in addition to neighboring cells. Moreover, on the 316L sample, as shown in Fig. 6a, cells were observed to grow on surface. In contrast, on the 316L with additions samples surface cell growth was less pronounced, with limited establishment of cell spreading being seen after 96 h days of culture. On the 316L sample cell numbers were increased, and the entire sample's surface was covered with cells having numerous filopodia extensions attached to the surface.

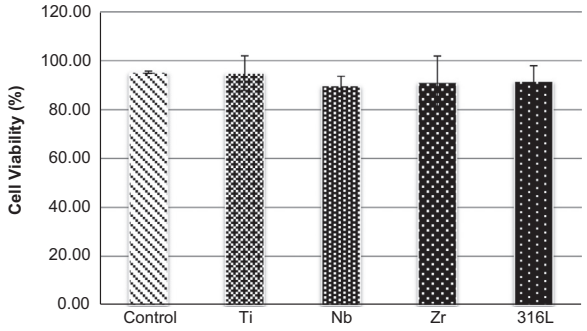


Fig. 8 – Effect of different additions of 316L on cell viability by Trypan blue assay in 96 h.

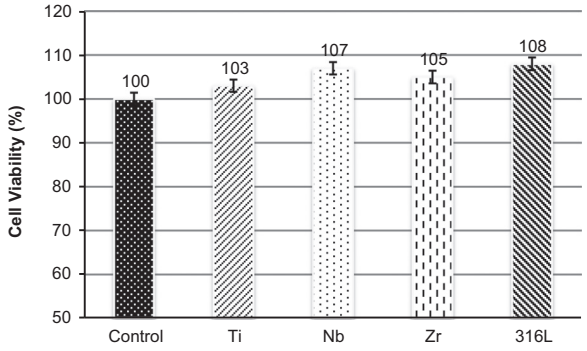


Fig. 9 – Effect of different additions of 316L on cell viability by MTT assay in 96 h.

Fig. 7 shows the phase contrast microscopic examination revealed not significant differences in the cell growth behavior for 96 h near the surfaces of 316L, 316L+Zr, 316L+Nb and 316L+Ti, respectively. Black areas at the corners of the photographs are the borders and shadows of the test samples. As shown in Fig. 7 for the 316L surface, the fibroblasts near the sample with the shape of shuttle and/or elongated polygon, which are the normal individual form of the 3T3 mouse fibroblast cells (Cui and Chen, 2008). Cells morphologies near the 316L additives were similar to those near the 316L, but the number of attached cells was slightly higher than that on 316L with Zr.

Fig. 8 shows the Trypan blue results of cell represented at the end of 96 h in all experimental groups. When compared test results, 316L with Ti is the best biocompatible alloy and all groups were very close to Ti and each other. Our cell culture data indicated that 316L with Ti, 316L with Nb and 316L with Zr stainless steels are biocompatible as 316L. Fig. 9 shows the MTT results of cell represented at the end of 96 h in all experimental groups. When compared to cell proliferation in metal containing groups, the 316L with Nb was slightly higher than other injected groups and also all groups are similar to each other and control groups.

4. Conclusions

The present study investigates the effect of Zr, Nb and Ti addition on the sintered density, mechanical, corrosion

properties and biocompatibility of injection molded 316L stainless steel. The overall mechanical and corrosion performance of injection molded 316L stainless steel and 316L with Zr, Nb and Ti additions correspondingly improves with increase in the sintering temperature. Mechanical, corrosion and SBF immersion tests and results show that the Ca-deficient apatite is bone-like apatite with excellent bioactivity. The 316L stainless steel with Zr, Nb and Ti addition materials are high strength and good bioactive materials and possess promising applications as biomedical materials. The results of cell culture show that 316L and 316L additives are well tolerated by the 3T3 mouse fibroblasts, which showed normal morphology and attached onto the samples over the incubation times. When the all properties of 316L and added samples compared, added samples have higher mechanical, corrosion and biocompatible properties. Considering all properties, Ti added 316L samples have much better properties.

Acknowledgments

This work was supported by the Scientific Research Project Program of Marmara University (Project number: FEN-E-130313-0079).

REFERENCES

Auzene, D., Jacquemin, T., Duval, J.L., Egles, C., Popot, J.M., 2014. Biological characterization of materials produced by powder injection moulding for dental applications. Powder Metall. 58 (1), 16–19.

Bayraktaroglu, E., Gulsoy, H.O., Gulsoy, N., Er, O., Kilic, H., 2012. Bio-Med. Mater. Eng. 22, 333–349.

Breme, J., Thull, R., Kirkpatrick, C.J., 2007. Metallic Biomaterial in Faces. Wiley-VCH, Weinheim125–130.

Cui, Z.D., Chen, M.F., 2008. Improving the biocompatibility of NiTi alloy by chemical treatments: an in vitro evaluation in 3T3 human fibroblast cell. Mater. Sci. Eng. 28, 1117–1122.

Dehoff, R.T., Rummel, R.A., Labuff, H.P., Rhines, F.N., 1966. The relationship between surface area and density in second-stage sintering of metals. In: Hausner, H.H. (Ed.), Modern Developments in Powder Metallurgy, vol. 1. Plenum Press, New York, NY, pp. 310–331.

Elter, P., Sickel, F., Ewald, A., 2009. Nanoscaled periodic surface structures of medical stainless steel and their effect on osteoblast cells. Acta Biomater. 5, 1468–1473.

Faghihi, S., Zia, S., Taha, M.F., 2012. Adipose tissue-derived stem cell response to the differently processed 316L stainless steel substrates. Tissue Cell 44, 365–372.

German, R.M., Bose, A., 1997. Injection Molding of Metals and Ceramics. MPIF, NJ55–60.

German, R.M., 1996. Sintering Theory and Practice. John Wiley & Sons, Inc, NY197–207.

Gulsoy, H.O., 2005. Influence of nickel boride additions on sintering behaviors of injection moulded 17-4 PH stainless steel powder. Scr. Mater. 52, 187–192.

Gulsoy, H.O., Ozbek, S., Baykara, T., 2007. Microstructural and mechanical properties of injection moulded gas and water atomized 17-4 PH stainless steel powder. Powder Metall. 50 (2), 120–126.

Gulsoy, H.O., 2008. Production of injection moulded 316L stainless steels reinforced with TiC(N) particles. Mater. Sci. Technol. 24 (12), 1484–1491.

Hong, Z.S., Hui, W.G., Zhong, Z.Y., 2005. Biocompatibility of MIM 316L stainless steel. J. Cent. South Univ. Technol. 12, 9–11.

Liu, B., Zheng, Y.F., 2011. Effects of alloying elements (Mn, Co, Al, W, Sn, B, C and S) on biodegradability and in vitro biocompatibility of pure iron. Acta Biomater. 7, 1407–1420.

Li, M., Yin, T., Wang, Y., Du, F., Zou, X., Gregersen, H., Wang, G., 2014. Study of biocompatibility of medical grade high nitrogen nickel-free austenitic stainless steel in vitro. Mater. Sci. Eng. C: Mater. Biol. Appl. 43, 641–648.

Nakamura, H., Toyoshime, H., Otsu, H., Chiba, A., Abe, K., 2011. Effect of a slight addition of Zr on the sintering behaviour of water-atomised 316L stainless steel powder. Powder Inject. Molding Int. 5, 60–66.

Park, J.H., Kim, J.K., Lee, B.H., Seo, H.S., Kim, K.Y., 2014. Effect of Zr addirion on intergranular corrosion of low-chromium ferritic stainless steel. Scripta Mater. 76, 77–80.

Parsapour, A., Khorasani, S., Fathi, M.H., 2013. Effect of surface treatment and metallic coating on corrosion behavior and biocompatibility of surgical 316L stainless steel implant. J. Mater. Sci. Technol. 28 (2), 125–131.

Shaw, N.J., 1989. Densification and coarsening during solid state sintering of ceramics: a review of the models. III. Coarsening. Powder Metall. Int. 21 (6), 25–29.

Suri, P., Koseski, R.P., German, R.M., 2005. Microstructural evolution of injection molded gas and Water atomized 316L stainless steel powder during sintering. Mater. Sci. Eng. A 402, 341–348.

Tang, Y.C., Katsuma, S., Fujimoto, S., Hiromoto, S., 2006. Electrochemical study of Type 304 and 316L stainless steels in simulated body fluids and cell cultures. Acta Biomater. 2, 709–715.

Velasco, F., Isabel, R., Anton, N., Martinez, M.A., Torralba, J.M., 2002. Composites A 33A (6), 819–827.

Wang, L., Zhao, X., Ding, M.H., Zheng, H., Zhang, H.S., Zhang, B., Li, X.Q., Wu, G.Y., 2015. Surface modification of biomedical AISI 316L stainless steel with zirconium carbonitride coatings. Appl. Surf. Sci. 340, 113–119.

Xin, F., Jian, C., Peng, Z.J., 2009. Bone-like apatite formation on HA/316L stainless steel composite surface in simulated body fluid. Trans. Nonferrous Met. Soc. China 19, 347–352.

Zhao, D., Chang, K., Ebel, T., Nie, H., Willumeit, R., Pyczak, F., 2015. Sintering behavior and mechanical properties of a metal injection molded Ti–Nb binary alloy as biomaterial. J. Alloy. Compd. 640, 393–400.